Hatem H. Obeid
University of Babylon, College of Engineering, Dep. of Mechanical Eng., Babylon, Iraq
eng.hatem.hadi@uobabylon.edu.iq

Riham A.Nima
University of Babylon, College of Engineering, Dep. Of Mechanical Eng., Babylon, Iraq

Received on: 05/04/2015
Accepted on: 19/05/2016

Published online: 25/01/2019

Investigation of Optimum Helix Angle of a Wire Rope Subjected to Harmonic Dynamic Loading

Abstract- *The current work includes the dynamic structural analysis of wire rope with different helix angle. The main objectives are; estimating the stress and deflection for each helix angle, comparing the results to get the best helix angle suitable for practical applications. This paper falls into two parts: The first part includes modal analysis for the models of wire rope using finite element method with certain boundary conditions that are suitable to obtain the first five frequencies for each helix angle and the second part focuses on harmonic analysis of wire rope to estimate stress and deflection and compares maximum results that coincide with the first natural frequency of each model. In the analysis the results of each helix angle were compared to other helix angle results, the structure of 82° helix angle have the smallest stresses and deflection. That means when the helix angle increases the flexibility decrease and rigidity increase.*

Keyword: *Simple straight strand, finite element model, modal analysis, harmonic analysis.*

How to cite this article: H.H. Obeid and R.A.Nima "Investigation of Optimum Helix Angle of a Wire Rope Subjected to Harmonic Dynamic Loading," *Engineering and Technology Journal*, Vol. 37, Part A, No. 1, pp. 6-11, 2019.

1. Introduction

During the past some years, many developments have been carried out in the steadying the responses of metal cables that formed as spiral strands and wire ropes. Strand can be defined as a set of wires fabricated in helical form in sequential layers over a straight central main wire. Typically wire rope element consists of six coils twisted over a central core. It is maybe consisting of twisted fiber or a smaller independent wire rope. The main difference between strand and wire rope is that the wires in a rope follow more complex doubly helical paths in strands that are fabricated into helices, while the individual wire rope in a spiral strand follows a simple twisted shape. Approximating methods were used for the dynamic analysis of the wire rope strand such as the finite element method, boundary element method in addition to the experimental techniques such as experimental modal analysis. The purposes of the dynamic analysis of strand are investigation its behavior under the action of dynamic excitations. Jiang et al. in [1] have been used finite element analysis of simple straight strand. Kastratović et al [2] have used advanced 3D modeling techniques and finite element method for wire rope strand analysis. İmrak and Erdönmez. N.F [3] have been studied using finite element analysis a realistic three dimensional structural model of a simple wire strand. Casey et al [4] have been investigated an introductory study into the ability to apply techniques of signal analysis to wire rope strand configurations. Etsujiro Imanishi et al. [5] have been studied the dynamic simulation of wire rope with contact. Wei-Xin Ren et al. [6] have been carried out a validated study by using finite element method with respect to environmental vibration test results to be served as the base for a more accurate dynamic responses investigation. Guohua CAO et al. [7] have been studied a numerical modelling and dynamic properties of hoisting rope used in roller wind system. In this paper, a comparative study is to be presented to investigate the optimal helix angle such that the strand withstands the effect of harmonic excitation. Finite element method is using to carry out this study such that two solutions including modal and frequency analysis are to be intended to reach to the objectives.

2. Strand Finite Element Models

The finite element method was used for the modeling of the wire rope strand under the action of dynamic excitations. The geometry of the wire rope strand is shown in Figure 1. The cross-section of a wire rope consists of one simple, straight, seven-wire strand. Such a cross-section is often used as a rope core in a more complex rope and as such is sometimes called an independent wire rope core or IWCR. It is consisting of multiple wires that hold the most value of the applied axial load. The mesh has been created using solid brick element

http://doi.org/10.30684/etj.37.1A.2
2412-0758/University of Technology-Iraq, Baghdad, Iraq

(SOLID186) in Ansys version 11 for 3D modelling of models of different helix angles. The software used in this study allows linear contacts; bonded contact is considered for simulation of contact. The core strand radius of centre wire was R1 = 1.97 mm, and outer wire R2 = 1.865 mm with different helix angle (74˚, 76˚, 78˚, 80˚, 82˚). The entire length of the wire rope model was (18 mm). Boundary conditions were assigned such that one end is constrained in all translations and rotations degrees of freedom while another end is free for translations and rotations. The elasticity modulus of the steel was taken as E = 2 E11 Pa, Poisson's ratio ν = 0.3 and damping ratio = 0.02 [2].

3. Modal analysis

The modal analysis was used for the estimation of the dynamic properties of the strand for each helix angle. The dynamic properties of the strand are included the natural frequencies and the normal (mode) shapes. Both of the natural frequencies and mode shapes are influenced by the stiffness and mass properties of the strand. Then the estimated natural frequencies are mathematically modeled with the effect of the helix angles. The governing differential equations of motion for the free vibration problem with the undamped case were assumed [9] is:

$$[M]\{\ddot{u}\}+[K]\{u\}=\{0\} \tag{1}$$

Assuming harmonic motion that is: $\{u_n\}=\{\phi_n\}\sin\omega_n t \quad ; \quad n=1,2,...N$ (2)

Where:

N is the D.O.F. of the model.

$\phi_n\}$ is the normal mode vector for the n^{th} mode.

ω_n is the angular natural frequency of mode n.

Differentiating Equation (2) twice with respect to time yields:

$$\{\ddot{u}_n\} = -\omega_n^2 \ \{\phi_n\}\sin \tag{3}$$

Then, substituting Equations (2), (3) into Equation (1) then multiplying by $\{\phi_n\}^T$ yields, after canceling the term

$$(\sin \omega_i t)\ ([K]-\omega_n^2[M])\{\phi_n\}\{\phi_n\}^T=\{0\} \tag{4}$$

Frequency equation (4) is of the form of the algebraic Eigen value problem (Kϕ=λMϕ). Nontrivial solutions have occurred if coefficient matrix determinant is equal to zero. Thus:

$$\left|[K]-\omega_n^2[M]\right|=\{0\} \tag{5}$$

The Characteristic equation will be obtained when extracting of the determinant to regression of n order. Characteristic values or Eigenvalues will be obtained for n roots of this regression (ω_n^2). The natural frequency (f_n) is then obtained from:

$$f_n= \omega_n / 2\pi \tag{6}$$

The characteristic vectors or the Eigenvectors $\{\phi_n\}$ will be obtained by Substitution of Eigenvalues (one at each time) into equation (6) within arbitrary constants. A number of solution algorithms have been developed for the solution of the Eigenvalue problem.

4. Harmonic Analysis

The Harmonic analysis was used for the analysis of the dynamic stresses and strains under action of periodic loading [9]. In harmonic analysis the time responses of each of deformations, stresses and strains are modelled in both frequency and time domains. The applied forces are formulated in frequency form to be assigned in the solution analysis in Ansis11. Forces can be in the form of applied loads and/or enforced motions (displacement, velocity or acceleration). The loading is defined in the solution as having an amplitude at a specific frequency. The steady-state oscillatory responses are occurring at the same frequency as the loading. The system is assumed subjected to a sine-wave periodically load p(t) of amplitude termed by p and excitation circular frequency $\overline{\omega}$, then the equation of motion is written as:

$$[M]\,\ddot{u}(t) + [c]\,\dot{u}(t)+[K]\,u(t) =\{p\} \sin \overline{\omega t} \tag{7}$$

Which is can be rewritten for N-uncoupled equations as:

$$\ddot{Y}(t) + [2\zeta_n\omega_n]\,\dot{Y}(t) + [\omega_n^2]\,Y(t)= \frac{P_n}{M_n} \sin \overline{\omega t} \tag{8}$$

n: 1,2,…….N

Then the induced deformations (displacements) can be obtained by the dot product of the normal mode vector (φ_n) and the modal amplitude (Y_n) as;

$$u_n = \varphi_n Y_n \tag{9}$$

$$M_n = \varphi_n^T\, m\, \varphi_n\ ,\ P_n= \varphi_n^T\, p \tag{10}$$

To continue with the solution of these uncoupled equations of motion, the Eigenvalue is solved first as:

$$[\bar{k} - \omega_n^2 m]\,\hat{u} = 0 \tag{11}$$

The normal modes φ_n (n= 1; 2; . . .), natural frequencies ω_n and modal damping ratios ζ_n are affecting the time response as:

$$Y_n(t) = \frac{1}{2\pi}\int_{-\infty}^{\infty} H_n(\overline{i\omega})\ P_n(\overline{i\omega})\exp \overline{i\omega}\, t\ d\overline{\omega} \tag{12}$$

In this equation, the complex load function $P_n(\overline{i\omega})$ is the Fourier transform of the modal loading $P_n(t)$ it is given by:

$$P_n(\overline{i\omega}) = \frac{1}{2\pi}\int_{-\infty}^{\infty} \mathrm{Pn(t)} \, \exp(-\overline{i\omega}\, t) \, dt \tag{13}$$

Also in Eq. (6), the magnification function, $H_n(\overline{i\omega})$, can be written as:

$$\mathbf{H_n}(\overline{\mathbf{i\omega}}) = \frac{1}{\omega_n^2 M_n}\left[\frac{1}{\left(\left(1-\beta_n^2\right) + i(2\zeta_n \beta_n)\right)}\right] = \frac{1}{\omega_n^2 M_n}\,\frac{\left[\left(\left(1-\beta_n^2\right) + i(2\zeta_n \beta_n)\right)\right]}{\left(\left(1-\beta_n^2\right)^2 + i(2\zeta_n \beta_n)^2\right)} \tag{14}$$

Where $\zeta_n \geq 0$

In these functions, $\beta_n = \frac{\overline{\omega}}{\omega_n}$ and $\omega_{Dn} = \omega_n \sqrt{1-\zeta_n^2}$. $\mathbf{H_n}(\overline{\mathbf{i\omega}})$ are Fourier transform pairs for the general principal loading leads to the principal response $Y_n(t)$ for $t \geq 0$. Also the initial conditions that termed by $Y_n(0)$ and $\dot{Y}_n(0)$ in this equation are estimated from the values of $u(0)$ and $\dot{u}(0)$ as;

$$\mathbf{Y_n}(0) = \frac{\varphi_n^T\, m\, u(0)}{\varphi_n^T\, m\, \varphi_n},$$

$$\dot{\mathbf{Y}}_n(0) = \frac{\varphi_n^T\, m\, \dot{u}(0)}{\varphi_n^T\, m\, \varphi_n}$$

The forced vibration response is given by [11]:

$$Y_n(t) = \left[Y_n(0)\cos \omega_{Dn} t + \left(\frac{\dot{Y}_n(0) + Y_n(0)\,\zeta_n\,\omega_n}{\omega_{Dn}}\right)\sin \omega_{Dn} t\right] \exp(-\zeta_n \omega_n t) \tag{15}$$

5. Result and Discussion

The structural natural frequencies were solved in the modal analysis for each helix angle. The solution take into account the variation of the structural stiffness for different helix angle, while maintain the mass of each model as a constant.The first five modes were considered for each helix angle. Table 1 shows the results of natural frequencies for the first five modes for each helix angle. It's obvious that the first natural frequency of the helix angle (80˚) was the largest value compared with other angles.

Table 1: Simple strand natural frequency

Natural Frequencies in Hz	first	second	third	fourth	fifth
Helix angle 74 ˚	1315.7	1360.8	1365.9	1805.5	1828.5
Helix angle 76 ˚	1321.4	1371.6	1374.5	1816.1	1838.6
Helix angle 78 ˚	1326.3	1380.2	1385.3	1824.8	1858.6
Helix angle 80˚	1332.5	1391.8	1393.1	1852.4	1867.9
Helix angle 82˚	1327.3	1382.7	1395.8	1864.6	1881.6

The structure with all helix angles were examined under action of harmonic load using harmonic analysis. The excitation load included a frequency domain within a range from zero to the third natural frequency.

Figures 2 and 3 show deflection of core and wire obtained from harmonic solution. We can see that the deflection of core is less than the deflection of wire, the maximum deflection was coinciding with the first natural frequency, a small deflection occurs at (82˚) helix angle.

Von mises stress was estimated at three locations along the model (upper, middle and lower) Figures 4-9 show the stresses in upper, middle, and lower locations of the core wire and helical wire respectively for all helix angles. The stress in upper location (fixed end) is the smallest while the stresses in middle location are larger than upper location and smaller than lower location, the stresses in core wire are less than stresses in the helical wire, for both core wire and helical wire, the helix angle (82˚) have the lowest stresses. One can see that the highest stress indicated at the first natural frequency. Figures (10-15) show shear stress at three locations (upper, middle, lower) along the model for each helix angle the largest shear stress was indicated at the middle location. The maximum strain coincides with the first natural frequency; Tables 2 and 3 show the average strain for core wire and helical wire that indicated with the first natural frequency.

Table 2: Harmonic strain of core wire

Helix angle	74 ˚	76˚	78˚	80˚	82˚
Strain -mm	1 $\times 10^{-3}$	9 $\times 10^{-4}$	5.3 $\times 10^{-4}$	4.3 $\times 10^{-4}$	4 $\times 10^{-4}$

Table 3: Harmonic strain of helical wire

Helix angle	74˚	76˚	78˚	80˚	82˚
Strain -mm	1.51 $\times 10^{-3}$	9.9 $\times 10^{-4}$	7.4 $\times 10^{-4}$	5.7 $\times 10^{-4}$	5 $\times 10^{-4}$

Note

The following symbols in figures denoted to helix angles
A =74 helix angle
B =76 helix angle
C = 78 helix angle
D = 80 helix angle
E = 82 helix angle

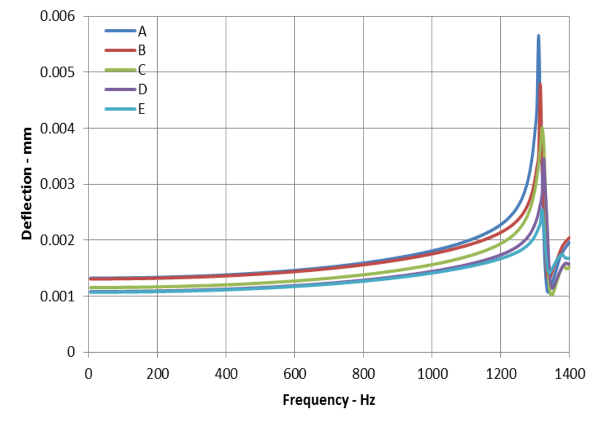

Figure 1: Harmonic deflection of core wire

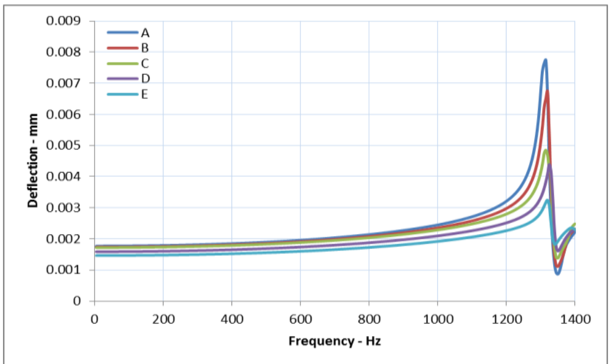

Figure 2: Harmonic deflection of helical wire

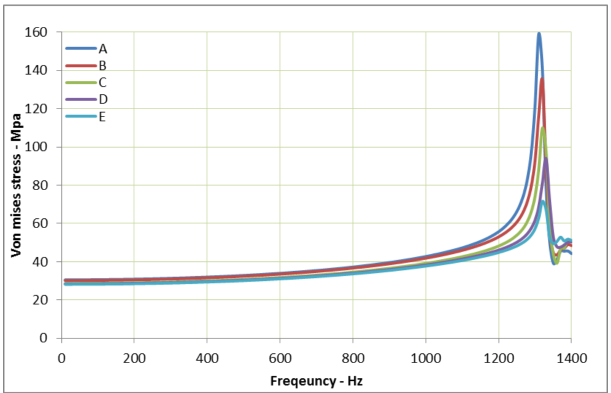

Figure 3: Harmonic von mises stress of core at upper location

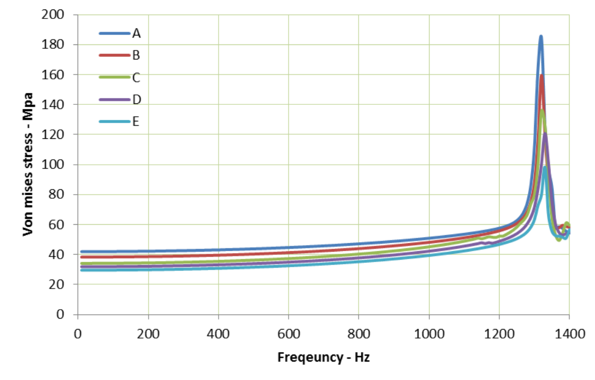

Figure 4: Harmonic von mises stress of core at middle location

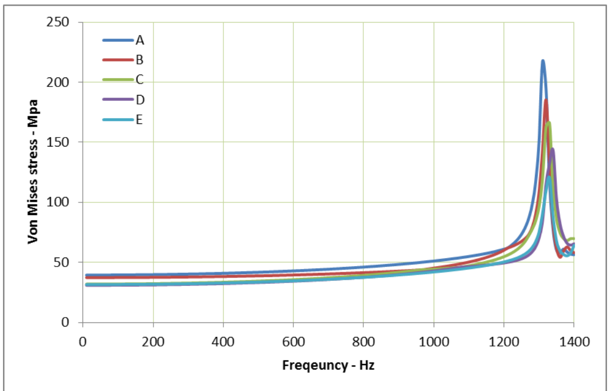

Figure 5: Harmonic von mises stress of core at lower location

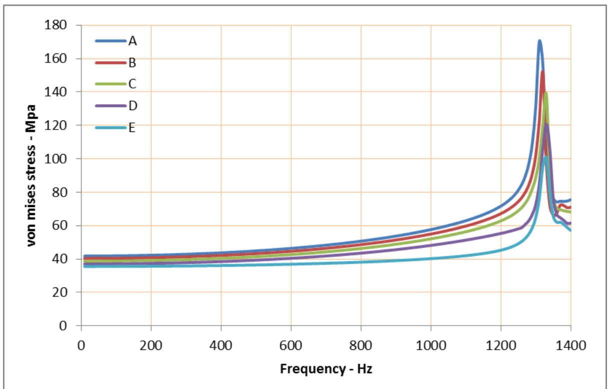

Figure 6: Harmonic von mises stress of helical wire at upper location

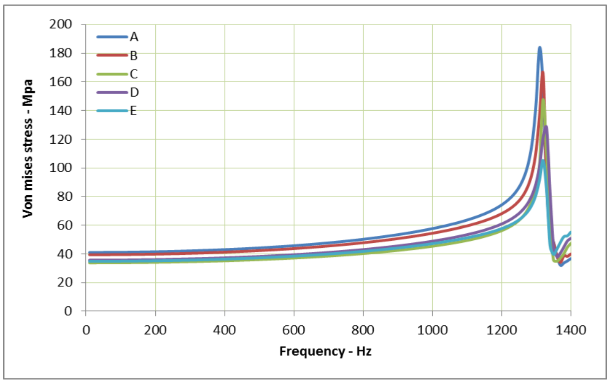

Figure 7: Harmonic von mises stress of helical wire at middle location

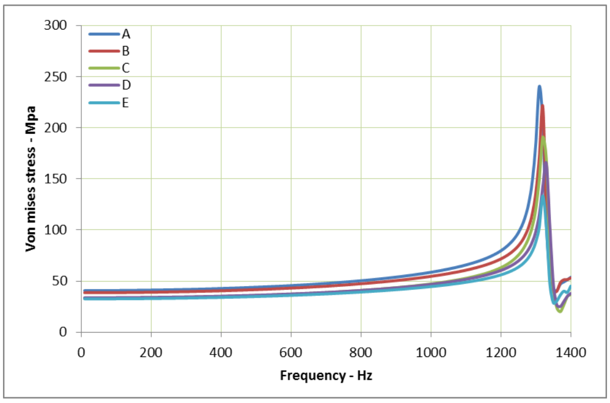

Figure 8: Harmonic von mises stress of helical wire at lower location

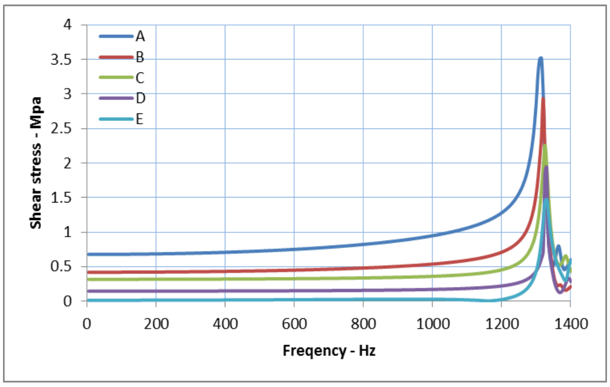

Figure 9: Harmonic Shear stress of core at upper location

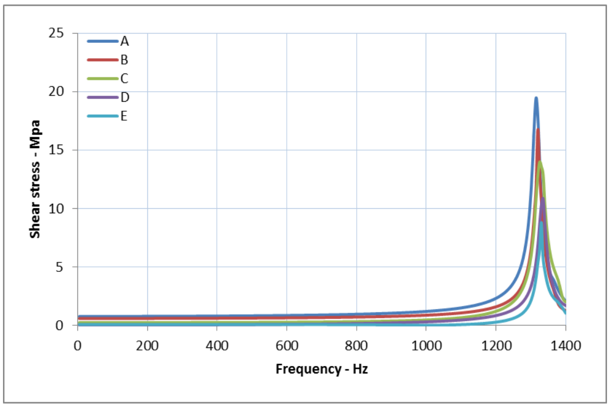

Figure 10: Harmonic Shear stress of core wire at mid location

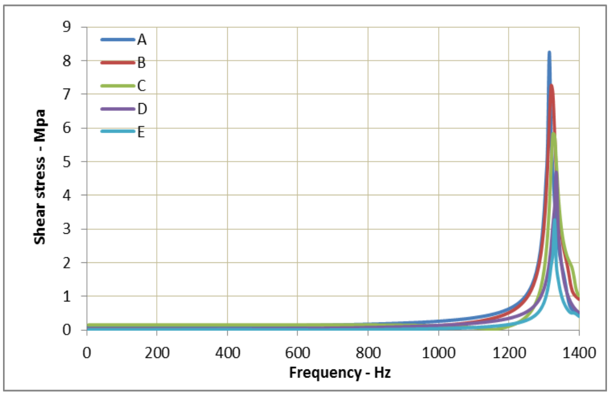

Figure 11: Harmonic Shear stress of core wire at lower location

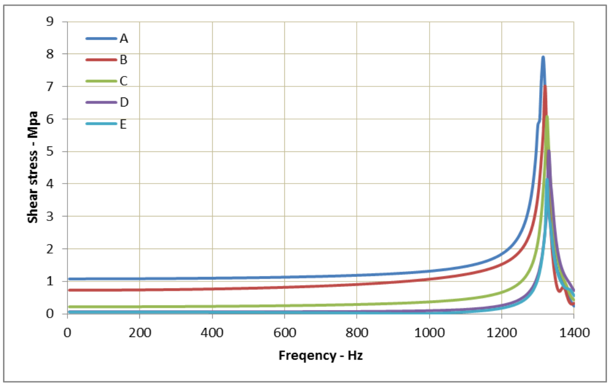

Figure 12: Harmonic Shear stress of helical wire at upper location

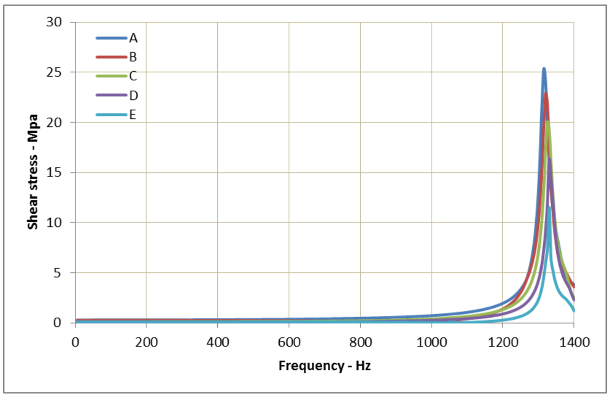

Figure 13: Harmonic Shear stress of helical wire at mid location

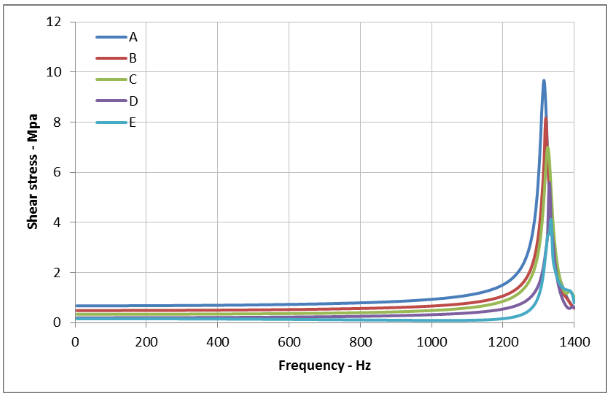

Figure 14: Harmonic Shear stress of helical wire at lower location

6. Conclusions

The structures of wire rope are analyzed by harmonic analysis, the location of peak value coincides with the first natural frequency and due to the fact that the frequency variation is depending on the helix angle so that the peak values differ. It is observed that the dynamical behaviour when the excitation frequency is near to or coincide on the first natural frequency is more dangerous than other frequencies, and then it must be avoided to ensure a safety state of structure. The structures of (82˚) helix angle are more withstanding periodic excitations since their response is smaller than the other helix angles.

References

[1] W.G. Jiang, J.L. Henshall and J.M. Walton, "A concise finite element model for three-layered straight wire rope strand," International Journal of Mechanical Sciences, Vol. 42, No. 1, pp. 63-86, 2000.

[2] G.M. Kastratović and N.D. Vidanović, "Some Aspects of 3D Finite Element Modeling of Independent Wire Rope Core," FME Transactions VOL. 39, No 1, 2011.

[3] C. Erdönmez and C.E. İmrak, "Modeling and numerical analysis of the wire strand," Journal of Naval Science and Engineering, Vol. 5, No. 1, pp. 30-38, 2009.

[4] N.F. Casey, H. White, and J.L. Taylor "Frequency analysis of the signals generated by the failure of constituent wires of wire rope," NDT INT. Vol 18. No- 6. Dec. 1985.

[5] E. Imanishi, T. Nanjo and T. Kobayashi "Dynamic simulation of wire rope with contact," Journal of Mechanical Science and Technology vol. 23, p 1083-1088, 2009.

[6] Wei Xin R, Xue Lin Peng, You Qin Lin "Experimental and analytical studies on dynamic characteristics of a large span cable-stayed bridge," Engineering Structures, Vol. 27, p 535–548, 2005.

[7] G. CAO, Z. ZHU, W. PENG & X. MAO, "Modelling and Natural Frequency Characteristics of Coupled Vibration with Varying Length of Hoisting Rope in Drum Winding System," Published in International Conference on Computing, Control & Industrial Engineering, 2010.

[8] S.F.A. Al-Wakel, M.R. Al-Qaissy and A.S. Abdulrasool, "Three-Dimensional Dynamic Analysis of Pile Foundations by Using Finite Element Method," Eng. & Tech. Journal, Vol. 33, Part (A), No.5, 2015.

[9] J.R. WilliamWeaver and P.R.Johnston, "Introduction to Structural Dynamic," Prentice-Hall, Inc., USA, 1987.

[10] Z.N.A. Al-Mousaoy, "Effect of Non-Linear Load Harmonics on Single phase Transformer Losses and Design Active Filter," Eng. & Tech. Journal, Vol. 29, No.11, 2011.

[11] R.W. Clough, Joseph Penzien, "Dynamics of Structures," Berkeley, CA 94704 USA, 1995.